JOURNAL OF CATALYSIS 83, 446–453 (1983)

Angular Distribution of the Desorption of CO_2 Produced on Well-Polished Polycrystalline Rhodium Surfaces

TATSUO MATSUSHIMA

Research Institute for Catalysis, Hokkaido University, Sapporo 060, Japan

Received March 16, 1983; revised May 13, 1983

The kinetics of the reaction of adsorbed CO with oxygen adatoms was studied on well-polished polycrystalline rhodium surfaces at low temperatures by means of angle-resolved thermal desorption. The CO_2 formation was observed as two peaks around 280 and 410 K. The angular distribution of the former varies as $(\cos\theta)^{\sim 8}$ and the other $(\cos\theta)^{\sim 5}$, where θ is the desorption angle. This difference is rationalized with an activation barrier model.

INTRODUCTION

The angular distribution of the desorption flux of product molecules gives microscopic insight into the dynamic behavior of surface reactions (*1, 2*). Recent work by Comsa's group (*3–6*) has shown that a simple one-dimensional model proposed by Willigen still can be used as a prototype model to explain the angular and velocity distribution of desorbing hydrogen molecules. This model, however, should be modified by considering several factors, i.e., the interaction between gas molecules and surfaces (*7, 8*), the vibrational modes of activated complexes (*9*), and potential energy profiles in the neighborhood of desorption sites (*10*). No theory has been successful in explaining in detail the velocity distribution. From the experimental point of view, it is important at present to investigate how the simple model fits (or does not fit) in with experimental results obtained in a wide range of experimental conditions.

The experimental procedures used to date for the angular distributions are either molecular beam scattering (*11*) or permeation experiments (*1, 12*). Both methods can be applied only at relatively high temperatures. Recently we have successfully used angle-resolved thermal desorption for analysis of the angular distribution of CO_2 produced on Pt(111) (*13, 14*). This method is useful for study over a wide coverage range of the reactants and at low temperatures. In addition, surface reactions which are started from stable coadsorption layers of the reactants can be studied.

The oxidation of carbon monoxide over catalysts from the platinum group metals has been investigated in numerous studies (*15*). Over Rh, CO_2 is produced from the interaction between CO admolecules and oxygen adatoms, i.e., the so-called Langmuir–Hinshelwood process (*16–19*). No microscopic kinetic studies on this system have been reported. In the present paper we will report the angular distribution of the desorption of CO_2 produced over well-polished polycrystalline Rh surfaces at low temperatures.

EXPERIMENTAL

Figure 1 shows a schematic diagram of the experimental apparatus. It consists of three ultra-high vacuum chambers; a reaction chamber, a collimator (*20*), and an analyzer chamber. They are separately pumped by individual ion pumps. The first has optics for LEED-AES, an Ar^+ gun, and a mass spectrometer. The collimator has two circular slits on both ends. The diameter of slit S1 is 2.7 mm and of S2, 4.0 mm. The former slit is 45 mm from the sample.

0021-9517/83 $3.00

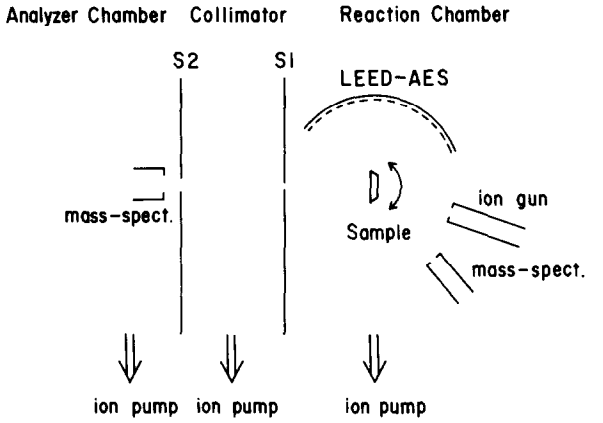

FIG. 1. Schematic diagram of the experimental apparatus.

The distance between the slits is 55 mm. The polycrystalline Rh sample was a disk-shaped slice (diameter 10 mm × thickness 0.8 mm). The purity was 99.99% from Furu-Uchi Chemicals (Japan). The crystal was polished with standard metallurgic techniques. It was set on a rotatable axis perpendicular to the axis of the collimator. It could be cooled down to 100 K and heated resistively. The sample was cleaned by repeated oxygen treatment and Ar^+ bombardment at 1000 K until a clean surface was obtained as judged by AES. The temperature was monitored by a chromel-alumel thermocouple spot-welded on the side. The sample was annealed to 1350 K before each run of thermal desorption.

Thermal desorption spectra were recorded in an angle-resolved form and also angle-integrated form with a mass spectrometer in the analyzer and reaction chamber, respectively. The signal monitored in the latter involves the contribution from the side of the sample crystal (ca. 14% of the total surface area) as well as from the well-polished surfaces. When the crystal is rotated away from normal an increasing area of the front face of the crystal falls inside the solid angle of acceptance of the apertures. A correction factor was computed for the experimental geometry and used when the relative value of the signal was determined as a function of the desorption angle.

RESULTS

In angle-resolved thermal desorption experiments, the catalyst surface is covered in advance by oxygen and CO, and then heated to produce CO_2. The product CO_2 leaving the surface which passes through the collimator is monitored with the mass spectrometer in the analyzer chamber. In order to survey the conditions suitable for such transient CO_2 production, several preliminary experiments were conducted.

Dependence of CO_2 Formation on CO and O_2 Exposure

The CO_2 formation spectra depended strongly on the amount of CO and O_2 exposure, adsorption temperature, and also exposure sequence. Throughout the present experiments oxygen was first dosed and then CO was introduced. CO_2 also could be produced by heating the sample exposed in the reverse order. In the latter case the observed CO_2 spectra were rather simple, and there was no separation of CO_2 peaks designated below as β_1 and β_2. When O_2 exposure was small, the resulting spectra had complicated structures. In the present work the surface was always preexposed to 1.2 ~ 1.4 L (Langmuir) of O_2. In this case CO_2 desorption only was observed at temperatures below 600 K. When O_2 pre-exposure was below 1 L, CO desorption could be observed in the temperature range 400–600 K.

Typical spectra (in the angle-integrated form) of the CO_2 formation with various exposures of CO are shown in Fig. 2. The surface was cooled down to 125 K and exposed to 1.4 L $^{18}O_2$ (the coverage relative to the saturation value determined by AES was 0.90). It was further exposed to various amounts of $C^{16}O$ (frequently oxygen-16 is simply designated as O) at the same temperature. Then it was heated with a constant current up to 1350 K. The temperature increased nearly linearly with a rate of 48 K/s below 800 K. The exposure pressure was always 2.4×10^{-8} Torr for $^{18}O_2$ and 1.0×10^{-8} Torr for CO. $C^{16}O^{18}O$ was produced over the wide temperature range 125–500 K. Neither $C^{16}O_2$ nor $C^{18}O_2$ was observed throughout the experiments. The $C^{16}O^{18}O$ formation started already below 150 K. A single peak (β_1) was observed around 330 K with small CO exposures. Above 0.5 L CO the spectrum became broad with an increase in CO exposure and showed a new peak β_2. A small shoulder of $C^{16}O^{18}O$ was also noticed around 150 K. It is indicated by an arrow in the figure. It appeared only when O_2 was predosed in large amounts. It was absent when the surface temperature was kept above 200 K during O_2 exposure. Therefore, this shoulder is likely to be due to α-CO_2, which is formed from the interaction between adsorbed CO and oxygen admolecules (*13, 14*). In fact oxygen can adsorb molecularly on Rh at 125 K (*21*). However, the amount of CO_2 in this shoulder was too small to be separated from the other, by using an isotope tracer technique (*14*).

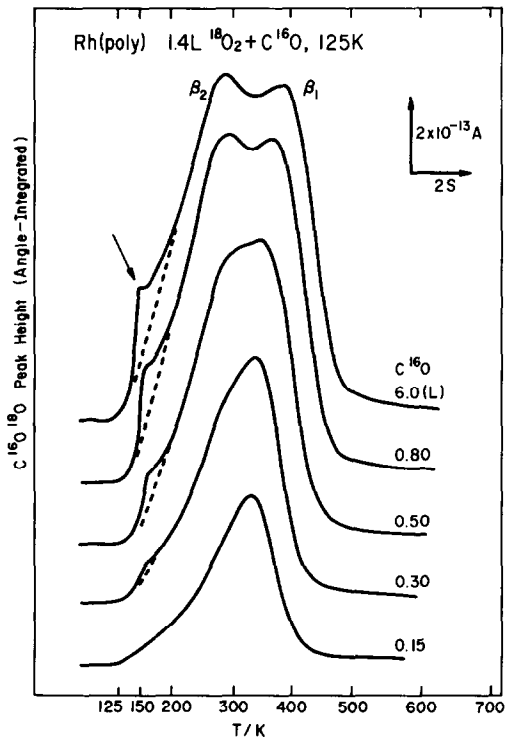

FIG. 2. CO_2 formation spectra with 1.4 L $^{18}O_2$ (the relative coverage 0.90) followed by various amounts of $C^{16}O$ exposure at 125 K. The heating rate was 48 K/s.

The separation of β_2 from β_1 became clearer when the surface temperature during O_2 exposure was raised. Typical examples are shown in Fig. 3. In this case the surface was exposed to 1.4 L $^{18}O_2$ at 200 K, and then to various amounts of $C^{16}O$ at 130 K. No changes in general features were observed. The small shoulder around 150 K disappeared. The better β_1–β_2 separation was quite reproducible. β-CO_2 is formed through the interaction between adsorbed CO and oxygen adatoms, since CO is molecularly adsorbed (*22, 23*) and oxygen is dissociatively adsorbed above 200 K (*21, 24*). Partial pressures of CO and O_2 were practically zero during CO_2 formation. This surface reaction for CO_2 formation may be first order in CO(a) and O(a). Second-order kinetics is expected. Therefore, the shift of the peak temperature of β_1 to higher values suggests nonuniform structures of coadsorption layers. The new β_2-CO_2 formation at low temperatures is reminiscent of a similar process on Pd(111) (*25*).

Angular Distribution of CO_2 Formation

Typical CO_2 formation spectra (in the angle-resolved form) with various CO exposures are shown in Fig. 4. These were recorded at the desorption angle $\theta = 0$. θ is the angle between the collimator axis and the surface normal. The surface was exposed to 1.4 L $^{18}O_2$ at 200 K and further to

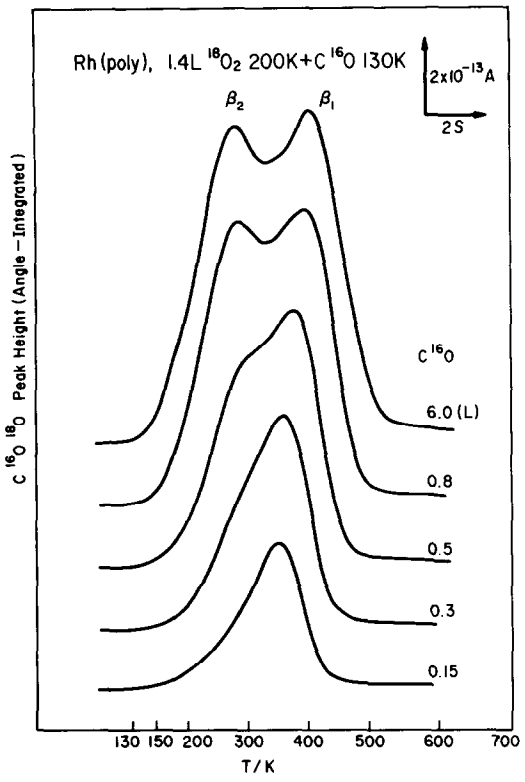

FIG. 3. CO_2 formation spectra with 1.4 L $^{18}O_2$ followed by various amounts of $C^{16}O$ exposure. $^{18}O_2$ was adsorbed at 200 K and $C^{16}O$ at 130 K. There is improved separation of β_1-CO_2 from β_2-CO_2. The heating rate was 48 K/s.

various amounts of $C^{16}O$ at 130 K. The amount of β_2-$C^{16}O^{18}O$ increases with CO exposure more rapidly than that in the angle-integrated form. Above 0.8 L of $C^{16}O$ the peak of β_2-$C^{16}O^{18}O$ is much higher than that of β_1-$C^{16}O^{18}O$. This fact indicates that the desorption of β_2-CO_2 is distributed along the surface normal more sharply than that of β_1-CO_2. Figure 5 summarizes typical CO_2 formation spectra observed at various desorption angles. The shape of the spectrum depends on the desorption angle. The dashed curves were drawn by assuming a constant half-width of the β_1-CO_2 peak independent of CO exposure. At large desorption angles the amount of β_2-CO_2 is comparable to that of β_1-CO_2. β_2-CO_2 becomes predominant with small desorption angles. This figure shows clearly that the angular distribution of β_2-CO_2 is sharper than that of β_1-CO_2. When CO exposure was small, only a single β_1 peak was observed. The relative peak height (after the correction due to surface area variation) of the β_1 peak is plotted against the desorption angle in Fig. 6. The angular distribution is very sharp along the surface normal. It varies as $(\cos\theta)^{6\pm1}$. The angular distribution with large CO exposures is shown in Fig. 7. In this case the surface was exposed to 1.4 L $^{18}O_2$ at 200 K and then to 1.2 L $C^{16}O$ at 125 K. Data above $\theta = 40°$ are rather scattered. The peak height of β_1-CO_2 varies as $(\cos\theta)^{5\pm2}$, while that of β_2-CO_2 as $(\cos\theta)^{8\pm2}$. The relative value of β_2-CO_2 always falls below that of β_1-CO_2. β_2-CO_2 shows a sharper angular distribution than that of β_1-CO_2.

For comparison, the adsorption of gaseous CO_2 and the angular distribution of the

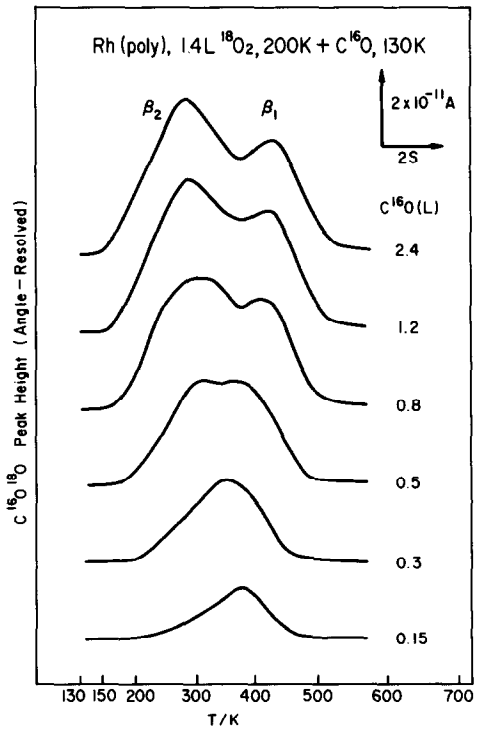

FIG. 4. CO_2 formation spectra observed in the normal direction. The surface was exposed to 1.4 L $^{18}O_2$ at 200 K and then to various amounts of $C^{16}O$ at 130 K. The heating rate was 48 K/s.

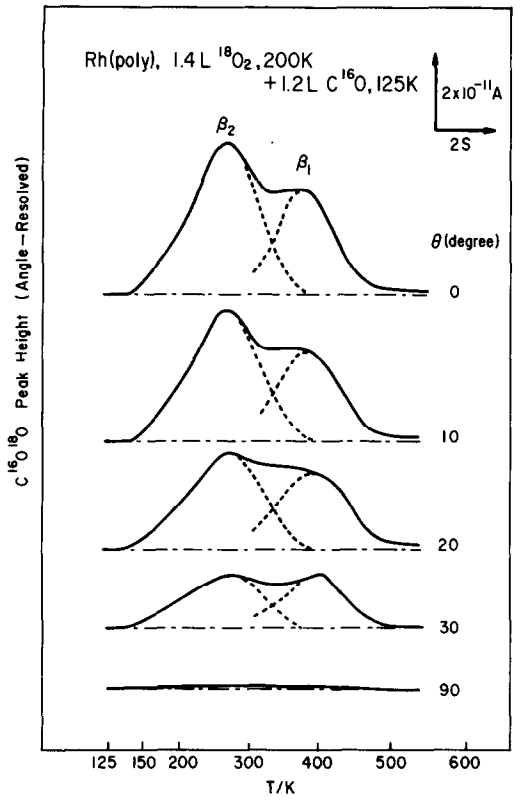

FIG. 5. CO_2 formation spectra observed at various desorption angles. The surface was exposed to 1.4 L $^{18}O_2$ at 200 K and then to 1.2 L C^{16}O at 125 K. The dashed curves were drawn with the assumption of a constant half-width. The heating rate was 42 K/s.

desorption flux were studied. CO_2 was dosed at 120 K. The desorption was complete below 150 K. The peak temperature of the desorption was 130 K. This is quite similar to that on Pt(111) (*14*). CO_2 could also be adsorbed on ^{18}O-covered surfaces. No oxygen exchange was observed between CO_2 adsorbed and ^{18}O(a). The peak temperature was almost the same as that on a clean surface. If CO_2 could be dissociated and produce CO(a) and O(a) on Rh (*22, 26*), the thermal desorption should produce a CO_2 signal around 300 K. No CO_2 signal was observed in the temperature range of CO_2 formation. It can be concluded that the interaction of CO_2 with a Rh surface is very weak, similar to the physisorption of CO_2 on Pt(111). The angular distribution of the desorption is shown in Fig. 8. It shows a simple cosine distribution, as expected for the desorption from a physisorption state (*27*).

DISCUSSION

In this section we will discuss the mechanism of the formation of β_1- and β_2-CO_2, and also their angular distributions.

Conrad *et al.* have found surface processes for CO_2 formation which behave quite similarly to β_1- and β_2-CO_2 in the present work. Those were observed on a Pd(111) surface highly covered by oxygen and then CO around 200 K (*25*). From LEED, UPS, and thermal desorption experiments, it was concluded that under certain conditions the adsorbates of CO and oxygen adatoms form separate domains and a true coadsorbate phase (cooperative adsorption), depending on the amount of

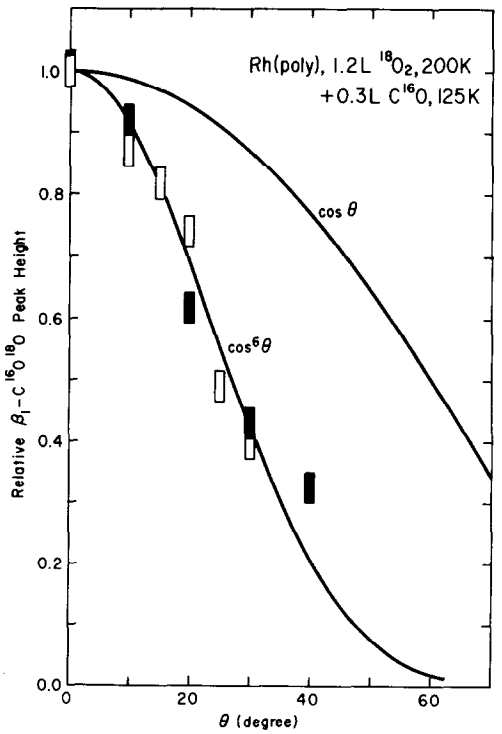

FIG. 6. Angular distribution of CO_2 formation with small CO exposures. The surface was exposed to 1.2 L $^{18}O_2$ at 200 K and then to 0.3 L C^{16}O at 125 K. The heating rate was 42 K/s.

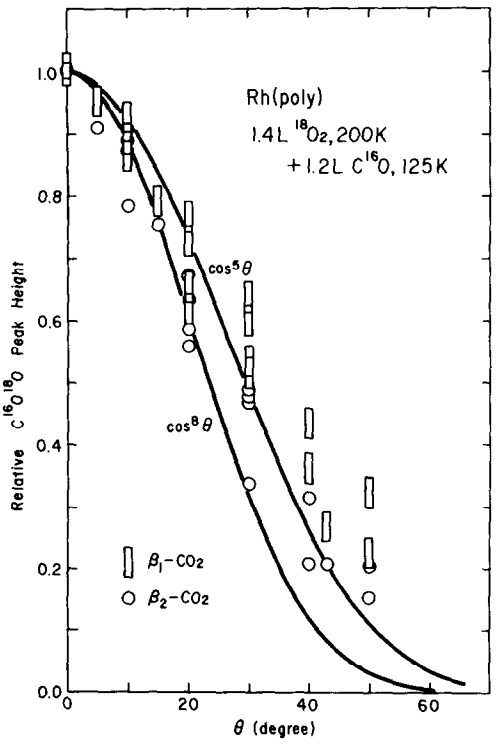

FIG. 7. Angular distribution of CO_2 formation with high CO exposures. The surface was exposed to 1.4 L $^{18}O_2$ at 200 K and then to 1.2 L $C^{16}O$ at 125 K. The heating rate was 42 K/s.

CO exposure. The former was produced by exposing an O(a)-saturated Pd surface to CO. The product CO_2 gave a thermal desorption peak in the temperature range 350–500 K. Further admission of CO at 200 K leads to the formation of regions consisting of a mixed phase of CO(a) and O(a). This cooperative adsorption layer is highly compressed and can produce CO_2 even at this temperature. The product CO_2 gave an additional thermal desorption peak below 300 K. This is quite similar to β_2-CO_2 in the present work. β_1-CO_2 can probably be assigned to the former.

β_2-CO_2 is produced in a dense coadsorbed layer. The potential energy of the initial state for β_2-CO_2 formation is likely to be raised above that for β_1-CO_2. The activation energy for the formation of β_2-CO_2 is lowered. A qualitative energy diagram for the CO_2 formation is shown in Fig. 9. CO_2 is adsorbed in the physisorption state. The potential energy of the initial state for CO_2 formation is the sum of the adsorption energy of CO(a) and O(a). Therefore, it is much lower than that of CO_2. When the surface is highly exposed to CO, the oxygen structure (probably (2 × 2) structure (*24*)) is compressed to the cooperative adsorption layer (*25*). The adsorption energy of CO and oxygen must be reduced significantly. The potential energy curve is shifted upward as shown with the dashed curve in Fig. 9. The activation energy for the CO_2

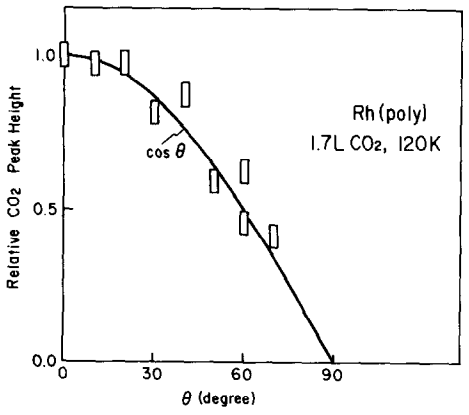

FIG. 8. Angular distribution of the flux of desorption of CO_2 adsorbed on clean Rh at 120 K. The surface was exposed to 1.7 L CO_2 at 120 K and heated at a rate of 17 K/s.

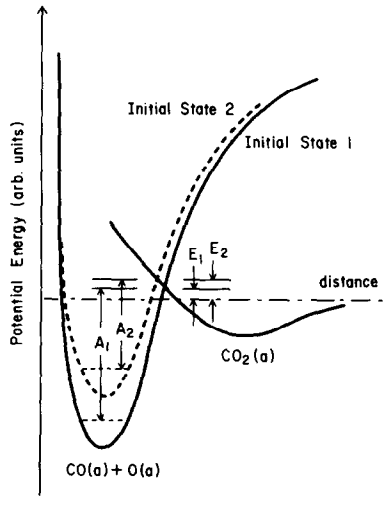

FIG. 9. Potential energy diagram for CO_2 formation.

formation is reduced from A_1 to A_2, so that CO_2 can be produced at lower temperatures. A zero point energy is drawn only for the initial states. A_1 (or A_2) is the difference between the zero point energy and the energy of the cross-point of the potential curve of the initial state and CO_2 physisorbed. This upward shift of the potential energy curve yields an increase in the energy of the activated complex at the cross-point relative to the vacuum level, from E_1 to E_2. This increment can produce a sharper angular distribution of CO_2 formation.

The desorption flux of CO_2 produced through the surface reaction shows an extremely sharp distribution along the surface normal. This fact indicates that the CO_2 molecule leaves the surface with an excess translational energy perpendicular to the surface. The molecule leaves the surface immediately after formation, without being trapped in the physisorption state. The origin of such an excess translational energy of desorbing molecules has typically been explained by a simple one-dimensional model proposed by Willingen (*1*). In this model the angular distribution is related to the activation barrier perpendicular to the surface for the *adsorption* or the energy of the activated complex relative to the vacuum level. This model should be modified by considering several factors as described in the Introduction. However, it is still useful to explain the general features of the angular distribution (*3–6*). The desorption rate at each angle is a function of the ratio, ε, of the activation energy relative to the vacuum level, E, to the thermal energy at the surface temperature, RT, as follows (*1*),

$$I(\theta) = I(\theta=0)\frac{\varepsilon + \cos^2\theta}{(\varepsilon + 1)\cos\theta} e^{-\varepsilon \tan^2\theta},$$

$$\varepsilon \equiv E/RT,$$

where $I(\theta)$ and $I(\theta = 0)$ are the desorption flux at $\theta = \theta$ and $\theta = 0$, respectively. From the angular distribution shown in Fig. 6, ε was estimated to be 3.0 for the curve of (cos θ)[6]. The peak temperature of CO_2 with 0.3 L CO was 330 K. E is roughly 2.0 kcal/mole. The value of E is 2.3 kcal/mole for β_2-CO_2, and 2.0 kcal/mole for β_1-CO_2 with large CO exposures. The value for β_2-CO_2 is definitively larger than that for β_1-CO_2. This is consistent with the prediction shown in Fig. 9. Although the discussion is limited in a qualitative sense, it can be shown that the angular distribution gives microscopic insight into the mechanism of the elementary steps involved in the surface reactions. Detailed discussion on the kinetics of the CO_2 formation will be published elsewhere, since more precise determination of the angular distribution and also analysis of the adsorption structures are in progress over single crystal surfaces.

ACKNOWLEDGMENT

This work was supported in part by a Grant-in-Aid for Scientific Research from the Ministry of Education, No. 554060.

REFERENCES

1. van Willigen, W., *Phys. Lett.* **28A,** 80 (1968).
2. Comsa, G., *Proc. 7th Intern. Vac. Congr. and 3rd Intern. Conf. Solid Surfaces (Vienna 1977)*, p. 1317.
3. Comsa, G., and David, R., *Chem. Phys. Lett.* **49,** 512 (1977).
4. Comsa, G., David, R., and Schumacher, B. J., *Proc. 4th Intern. Conf. Solid Surfaces and 3rd Eur. Conf. Surface Sci. (Cannes 1980)*, p. 252.
5. Comsa, G., David, R., and Schumacher, B. J., *Surface Sci.* **95,** L210 (1980).
6. Comsa, G., and David, R., *Surface Sci.* **117,** 77 (1982).
7. Schaich, W. L., *Phys. Lett.* **64A,** 133 (1977).
8. Doyen, G., *Proc. 4th Intern. Conf. Solid Surfaces and 3rd Eur. Conf. Surface Sci. (Cannes 1980)*, p. 145.
9. Toya, T., Ohno, Y., Ishi, S., and Nagai, K., *Proc. 4th Intern. Conf. Solid Surfaces and 3rd Eur. Conf. Surface Sci. (Cannes 1980)*, p. 141.
10. Horton, D. R., Banholzer, W. F., and Masel, R. I., *Surface Sci.* **116,** 22 (1982).
11. Palmer, R. L., and Smith, J. N., Jr., *Catal. Rev.* **12,** 297 (1975).
12. Comsa, G., David, R., and Schumacher, B. J., *Surface Sci.* **85,** 45 (1979).
13. Matsushima, T., *Surface Sci.* **123,** L663 (1982).
14. Matsushima, T., *Surface Sci.* **127,** 403 (1983).
15. Engel, T., and Ertl, G., *Adv. Catal.* **28,** 1 (1979).

16. Campbell, C. T., and White, J. M., *J. Catal.* **54,** 289 (1978).
17. Campbell, C. T., Shi, S-K., and White, J. M., *J. Vacuum Sci. Technol.* **16,** 605 (1979); *J. Phys. Chem.* **83,** 2255 (1979).
18. Campbell, C. T., Shi, S-K., and White, J. M., *Appl. Surface Sci.* **2,** 382 (1979); Kim, Y., Shi, S-K., and White, J. M., *J. Catal.* **61,** 374 (1980).
19. Matsushima, T., *J. Catal.* **64,** 38 (1980).
20. Kobayashi, M., and Tuzi, Y., *J. Vacuum Sci. Technol.* **16,** 685 (1979); Kobayashi, M., Kim, M., and Tuzi, Y., *Proc. 7th Intern. Vac. Congr. and 3rd Intern. Conf. Solid Surfaces* **2,** 1023 (1979).
21. Matsushima, T., unpublished data.
22. Dubois, L. H., and Somorjai, G. A., *Surface Sci.* **91,** 514 (1980).
23. Yates, J. T., Jr., Williams, E. D., and Weinberg, W. H., *Surface Sci.* **91,** 562 (1980); **115,** L93 (1982).
24. Thiel, P. A., Yates, J. T., Jr., and Weinberg, W. H., *Surface Sci.* **82,** 22 (1979).
25. Conrad, H., Ertl, G., and Küppers, J., *Surface Sci.* **76,** 323 (1978).
26. Dubois, L. H., and Somorjai, G. A., *Surface Sci.* **88,** L13 (1979).
27. Hurst, J. E., Becker, C. A., Cowin, J. P., Janda, K. C., Wharton, L., and Auerbach, D. J., *Phys. Rev. Lett.* **43,** 1175 (1979).